Solid State Communications 151 (2011) 1182–1187

Contents lists available at ScienceDirect

Solid State Communications

journal homepage: www.elsevier.com/locate/ssc

# Complex impedance spectroscopy of Mn-doped zinc oxide nanorod films

M.K. Sharma [a], R.N. Gayen [b], A.K. Pal [b], D. Kanjilal [c], Ratnamala Chatterjee [a,*]

[a] Magnetics and Advanced Ceramics Laboratory, Department of Physics, Indian Institute of Technology Delhi, New Delhi 110016, India

[b] Department of Instrumentation Science, USIC Building, Jadavpur University, Calcutta 700 032, India

[c] Inter University Accelerator Centre, Aruna Asaf Ali Marg, New Delhi 110067, India

ARTICLE INFO

*Article history:*
Received 7 December 2010
Received in revised form
18 March 2011
Accepted 27 April 2011
by D.D. Sarma
Available online 20 May 2011

*Keywords:*
A. ZnO nanorods
B. Mn doping
D. Impedance spectroscopy
D. X-ray photoelectron spectroscopy

ABSTRACT

The frequency-dependent properties of Mn-doped (3–5 at.%) aligned zinc oxide (Mn–ZnO) nanorods, synthesized by hybrid wet chemical route onto glass substrates, were investigated by bias-dependent impedance spectroscopy. No peak of Mn cluster/secondary phases was detected in the X-ray diffraction traces of the samples. XPS studies show the presence of oxygen vacancies in Mn–ZnO nanorods and Mn in $Mn^{2+}$ and $Mn^{4+}$ charge states. Although X-ray diffraction/X-ray photoelectron spectroscopy does not give any indication of the presence of metal clusters in the samples, bias-dependent impedance spectroscopy demonstrates significant sensitivity to the formation of Mn clusters in Mn–ZnO nanorods.



## 1. Introduction

There has been great excitement in reporting ferromagnetism with Curie temperature well above room temperature in transition metal (TM) doped diluted magnetic semiconductors (DMSs) or insulating oxides for advanced spintronic applications [1]. Transition metal doping into ZnO, $TiO_2$, $SnO_2$, or $HfO_2$ showed room temperature ferromagnetism [2–5], and the presence of defects or cation/oxygen vacancies [6–8] in materials in thin film form was associated with the magnetism observed in the systems concerned.

A key method for realizing a good DMS structure is to substitute the magnetic ions in the matrix of metal oxides and accordingly suppress the formation of magnetic clusters/secondary phases. Thus an important aspect of research in this field is to identify whether or not the large magnetization behavior in the sample is due to magnetic clusters. The existence of magnetic clusters in host materials is often difficult to detect by X-ray diffraction (XRD) or transmission electron microscopy (TEM), due to the fact that the size of the clusters is of the order of sub-nanometers. The sub-nanometer sized clusters also go undetected in temperature-dependent magnetization measurements as the blocking temperature ($T_B$) decreases with decreasing size of clusters, and thus may exceed the low temperature measurement limit of SQUID magnetometer systems [9].

It is known that the electrical properties of materials depend on different contributions from various components of the material. Overall properties of the host dielectric medium would be modulated by intra-grain and inter-grain defects, if any, and through electrode processes at higher temperatures (>800 K). The relaxation time ($\tau = RC$) or frequency response of complex impedance is known to provide evidence to identify various electrical relaxation mechanisms, arising from grains, grain boundaries, or macroscopic inhomogeneities in the form of equivalent circuit analysis [10,11]. Huang et al. [12] have recently shown that bias-dependent impedance spectroscopy may be a useful tool to detect the presence of magnetic clusters in transition-metal-doped ZnO films.

The ferromagnetic behavior of the Mn–ZnO nanorods under study may arise due to (i) dilute magnetic structure, (ii) lattice defects, (iii) secondary phase, or (iv) clustering of transition metal dopants. The aim of this work is to use complex impedance spectroscopy as a tool for probing the cause of ferromagnetism observed in these Mn–ZnO nanorods.

## 2. Experimental details

Vertically aligned ZnO nanorods were deposited by wet chemical route onto glass substrates on which ZnO seed particles were pre-deposited by the sputtering technique. Thus, this technique is essentially a hybrid technique, where one may easily

* Corresponding author.
*E-mail addresses:* rmala@physics.iitd.ac.in, ratnamalac@gmail.com (R. Chatterjee).

0038-1098/$ – see front matter © 2011 Elsevier Ltd. All rights reserved.
doi:10.1016/j.ssc.2011.04.028

manipulate the size and the distribution of ZnO seed crystallites. It should be clarified that although ZnO grows preferentially (in nanorod form) over the ZnO seed particles, during the chemical deposition process, modulating growth of ZnO over the whole substrate is expected. However, due to the presence of ZnO seed particles, the ZnO is shown to preferentially deposit as nanorods on these seed sites. The thickness of the chemically deposited ZnO film on the rest of the substrate would be negligible as compared to the nanorod length. Details of the synthesis of the above ZnO nanorods are reported elsewhere (Ref. [13] and reference therein).

Mn was evaporated on the ZnO nanorods at a system pressure $\sim 10^{-6}$ mbar for three different durations so as to deposit Mn layer with thickness ~3 nm, ~6 nm and ~10 nm keeping the rate of evaporation fixed at ~0.2 nm/s. The amount of manganese was controlled and recorded by a quartz crystal thickness monitor. The ZnO nanorods containing manganese, thus obtained, were then subjected to rapid thermal annealing (RTA) in argon atmosphere for dispersing Mn in ZnO nanorods. The temperature of annealing was 773 K and duration was 3 min. After annealing, the final composition of the films as estimated by X-ray photoelectron spectroscopy data, were found to be ~3 at.%, ~4 at.% and ~5 at.% for 3 nm, 6 nm and 10 nm Mn-deposited ZnO nanorod films, respectively.

An FEI Quanta 200 scanning electron microscopy (SEM) was used to record the surface morphology at an operating voltage of 25 kV in back scatter mode. A Rigaku MiniFlex X-ray diffraction (XRD) using Cu $K_\alpha$ radiation was used to obtain the structural information. The XPS spectra were recorded using a VG Microtech at a base pressure $\sim 10^{-10}$ mbar. The XPS setup used here is incorporated with a dual anode Mg–Al X-ray source with a hemispherical analyzer and a channeltron detector with a resolution 1.3 eV. Monochromatic Mg $K\alpha$ radiation (1253.6 eV) was used at 300 W for our XPS measurements. Data analysis was done using VGX900 software incorporated with the system.

The complex impedance spectroscopy was carried out using Agilent 4294 A impedance analyzer with two point contacts in a frequency range from 100 Hz to 20 MHz and a fixed oscillating voltage 500 mV under dc bias voltage $V_{dc}$ from 0 to 1.5 V. The geometry in which the measurement is done (i.e., two probes attached to the top of the sample) takes care of the impedance contributions from complete sample including nanorods and layer deposited on substrate during chemical deposition. By applying a dc bias voltage the relaxation contribution from different structural origin can be clearly identified.

## 3. Results and discussion

The SEM pictures of ~3 at.%, ~4 at.% and ~5 at.% Mn-doped ZnO nanorods are shown in Fig. 1. XRD traces of the as-deposited and annealed Mn–ZnO nanorods are shown in Fig. 2(a)–(f), respectively for all samples. XRD trace show that the vertically aligned ZnO nanorods are polycrystalline and preferentially [002] direction oriented. It may be noted that the characteristic peak for Mn (111) present in the XRD traces of the as-deposited films were masked due to the presence of very strong (002) peak of ZnO nanorods and hence in Fig. 2 the truncated (002) peak of ZnO is shown so as to reveal the (111) Mn peak located at $2\theta \sim 22.1^\circ$. It may be observed that no distinct peaks for Mn are observed in ZnO nanorods containing ~3 at.% Mn. As Mn concentration increases, Mn (111) peak at $2\theta \sim 22.1^\circ$ evolve more clearly in the XRD traces (Fig. 2(c) and (e)). It should be noted that after RTA, none of the samples show Mn (111) peak, indicating homogeneously distributed Mn in the ZnO matrix without affecting the observed vertical alignment of the ZnO (see Fig. 2(b), (d) and (f)). Lattice constants, a and c, of the Mn–ZnO nanorod films were computed using computer software package 'XPowder' [14] for the annealed

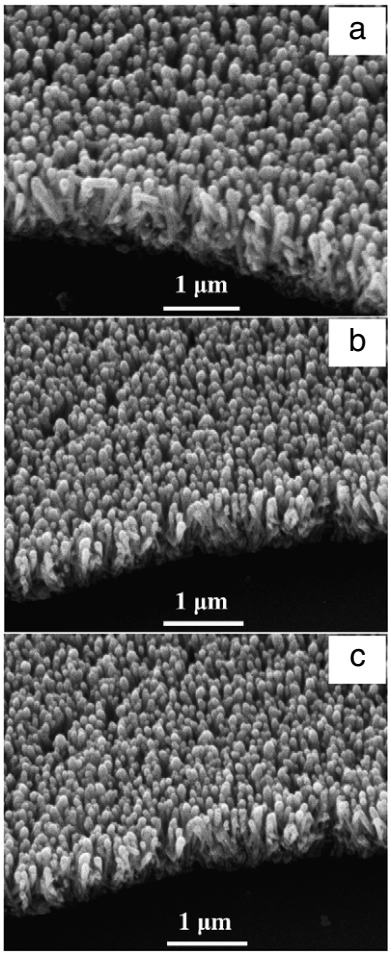


**Fig. 1.** SEM pictures of Mn–ZnO nanorod films with different amount of Mn: (a) Mn ~ 3 at.%; (b) Mn ~ 4 at.%; and (c) Mn ~ 5 at.%.

**Table 1**
Calculated lattice parameters (in nm), percentage of $Mn^{2+}$, Mn/Zn ratio and Zn/O ratio for Mn–ZnO nanorod films with different amount of Mn: (i) Mn ~ 3 at.%; (ii) Mn ~ 4 at.%; and (iii) Mn ~ 5 at.%.

| Sample | Lattice constants | Percentage of $Mn^{2+}$ | Mn/Zn | Zn/O |
|---|---|---|---|---|
| ZnO | $a \sim 0.324$<br>$c \sim 0.519$ | | | |
| Mn–ZnO (Mn ~ 3 at.%) | $a \sim 0.326$<br>$c \sim 0.519$ | 3 | 0.133 | 0.428 |
| Mn–ZnO (Mn ~ 4 at.%) | $a \sim 0.326$<br>$c \sim 0.519$ | 4 | 0.194 | 0.547 |
| Mn–ZnO (Mn ~ 5 at.%) | $a \sim 0.325$<br>$c \sim 0.519$ | 5 | 0.244 | 0.525 |

films and are shown in Table 1. It may be seen that the lattice constants agreed well with the bulk values ($a = 0.32495$ nm; $c = 0.52069$ nm) [15]. Results included in this communication hereinafter would relate to the rapid thermal annealed Mn–ZnO nanorod films, unless otherwise stated.

The binding states of the compositional elements of Mn–ZnO nanorods were characterized by XPS studies. Fig. 3(a)–(c) show the typical core level peaks corresponding to Zn 2p, O 1s and Mn 2p of the Mn–ZnO nanorods with increasing amount of Mn incorporated in them. The Mn $2p_{3/2}$ peak of Mn–ZnO nanorods located at 643.2 eV could be deconvoluted in two peaks located at ~641.4 and 643.3 eV, which could be attributed to the existence $Mn^{2+}$ and $Mn^{4+}$, respectively [16]. It is well known that, for one kind of element, ion with high valency has a larger binding energy. Generally, peaks for the metallic Mn and $Mn^{4+}$ ion are located at